

Detecting Adversarial Examples Based on Steganalysis

Jiayang Liu^a, Weiming Zhang^{a,*}, Yiwei Zhang^a, Dongdong Hou^a, Yujia Liu^a,
Nenghai Yu^a

^a*School of Information Science and Technology, University of Science and Technology of
China, No.96 Jinzhai Road, Hefei City, Anhui Province*

Abstract

Deep Neural Networks (DNNs) have recently led to significant improvement in many fields, such as image classification. However, these machine learning models are vulnerable to adversarial examples which can mislead machine learning classifiers to give incorrect classifications. Adversarial examples pose security concerns in areas where privacy requirements are strict, such as face recognition, autonomous cars and malware detection. What's more, they could be used to perform an attack on machine learning systems, even if the adversary has no access to the underlying model. In this paper, we focus on detecting adversarial examples. We propose to augment deep neural networks with a detector. The detector is constructed by modeling the differences between adjacent pixels in natural images. And then we identify deviations from this model and assume that such deviations are due to adversarial attack. We construct the detector based on steganalysis which can detect minor modifications to an image because the adversarial attack can be treated as a sort of accidental steganography.

Keywords: Adversarial examples, perturbation detection, deep neural network, steganalysis

*Corresponding author

Email addresses: ljyljy@mail.ustc.edu.cn (Jiayang Liu), zhangwm@ustc.edu.cn (Weiming Zhang), zywwvd@mail.ustc.edu.cn (Yiwei Zhang), houdd@mail.ustc.edu.cn (Dongdong Hou), yjcaihon@mail.ustc.edu.cn (Yujia Liu), ynh@ustc.edu.cn (Nenghai Yu)

1. Introduction

Deep Neural Networks (DNNs) have recently led to significant improvement in many fields, such as image classification [1, 2] and speech recognition [3]. DNNs are used for privacy protection in many scenes, such as identifying privacy-sensitive objects for image sharing [4], detecting and blurring faces or license plates in street view [5] and malware classification [6]. However, the generalization properties of the DNNs have been recently questioned because these machine learning models are vulnerable to adversarial examples [7]. An adversarial example is a slightly modified sample that is intended to cause a machine learning classifier to misclassify it. It's a critical risk that an attacker produces an image that has an incorrect, high confidence prediction with low distortion from a desired image, and human eyes can't perceive the distortion. In the context of classification, adversarial samples are crafted to force a target machine learning model to classify them in a class different from their legitimate class. In addition, adversarial examples have cross-model generalization property [8], so the attacker can even generate adversarial examples without the knowledge of the DNN. This kind of attack is particularly horrible in systems where privacy requirements are strict.

There are many studies which focus on methods of generating adversarial examples. Some attack methods are based on calculating the gradient of network, such as Fast Gradient Sign Method (FGSM) [8], Fast Gradient Value (FGV) [9], Jacobian Saliency Map Attack (JSMA) [10]. In addition, some methods are based on solving optimization problems, such as L-BFGS [7], Deepfool [11], Carlini & Wagner (C&W) attack [12].

Many defenses are proposed to mitigate adversarial examples against above attacks. They make it harder for the adversary to craft adversarial examples using existing techniques or make the DNNs still give correct classifications on adversarial examples. These defenses are mainly divided into two categories. One way is preprocessing the input image before classification, taking advantage of the spatial instability of adversarial examples. Defenders can perform

some operations on the input image in spatial domain before giving the input image to a DNN, such as JPEG compression, scaling, adding noise, etc. Gu et al. [13] proposed to use an autoencoder to remove adversarial perturbations from inputs. The other way is to modify the network architecture, the optimization techniques or the training process. Goodfellow et al. [8] proposed to augment the training set with adversarial examples to increase the models robustness against a specific adversarial attack. However, this approach faces difficulties because the dimension of the images and features in networks means an unreasonable quantity of training data is required. Zheng et al. [14] proposed to append a stability term to the objective function to force the model to have similar outputs for clean images of the training set and their adversarial examples. This is different from data augmentation because it encourages the smoothness of the model output between original and adversarial samples. Defensive distillation [15] is another technique against certain adversarial attacks. This form of network can prevent the model from fitting too tightly to the original data. Rozsa et al. [16] performed an experiment on the cross-model adversarial portability to show that models with higher accuracies tend to be more robust against adversarial examples.

Some researchers have proposed to build a network that detects and rejects an adversarial example. Metzen et al. [17] proposed to add a detection subnetwork which observes the state of the original classification network, one can tell whether it has been presented with an adversarial example or not. However, this approach is again vulnerable to counter-counter measures. In addition, the experiments of this technique were performed on 10-class ImageNet dataset not on the full 1000-class ImageNet dataset. So the performance of this technique on ImageNet-1000 is not known. Lu et al. [18] hypothesized that adversarial examples produce different patterns of ReLU activations in networks than what is produced by normal images. Based on this hypothesis, they proposed the Radial Basis Function SVM (RBF-SVM) classifier which takes advantage of discrete codes computed by the late stage ReLUs of the network to detect adversarial examples on CIFAR-10 and ImageNet-1000.

In this paper, we focus on detecting adversarial examples because the above detection methods are not meticulous enough. Our detection method draws on the idea of steganalysis which can detect minor modifications to an image. What’s more, we propose that adversarial examples can be detected by the classifier based on steganalysis because the adversarial attack can be treated as a sort of accidental steganography [7]. Our detection method exploits the fact that perturbation of pixel values by adversarial attack alters the dependence between pixels. By modeling the differences between adjacent pixels in natural images, we identify deviations from this model and assume that such deviations are due to adversarial attack. The detector is constructed as follows. A filter suppressing the image content and exposing the adversarial perturbation is applied. The dependence between neighboring pixels of the filtered image is modeled as a high-order Markov chain. The sample transition probability matrix is then used as a vector feature for a feature-based detector implemented using machine learning algorithms. In this way, it is difficult to attack the image classification network and the detector at the same time. Moreover, we propose a framework of defense mechanism against adversarial examples. First of all, we use our detector to detect the input image. If it is a normal image, we will directly feed it to the neural network to get the correct classification. Otherwise we can take advantage of the above defenses to mitigate adversarial examples.

2. Adversarial Attacks And Defenses

2.1. Attacks

2.1.1. Fast Gradient Sign Method(FGSM)

Goodfellow et al. [8] proposed the fast gradient sign method for generating adversarial examples. This method uses the derivative of the loss function of the model pertaining to the input feature vector. Given the input image X , the fast gradient sign method is to perturb the gradient direction of each feature by gradient. Then the trained networks classification of the input image has been changed. For a model with cross-entropy cost function $J(X, y)$ of the neural

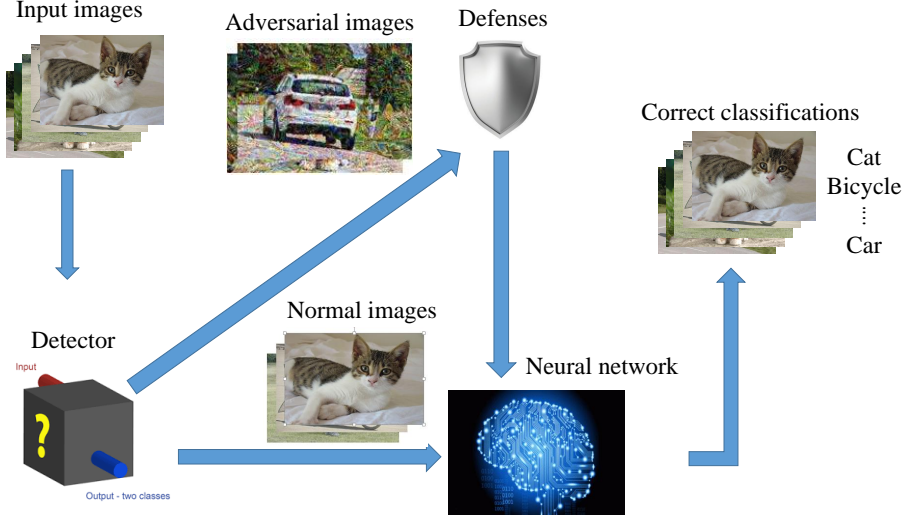


Figure 1: Framework of defense mechanism.

network, X is the input image, and y_t is the target class for the input image, the adversarial example is generated as

$$X^{adv} = X - \epsilon \text{sign}(\nabla_X J(X, y_t))$$

where ϵ is a parameter to determine the perturbation size.

2.1.2. Iterative Gradient Sign Method(IGSM)

The iterative gradient sign method is the iterative version of the fast gradient sign method. This method applies the fast method many times with small perturbation size instead of applying adversarial noise with one large perturbation size. The adversarial example of the iterative gradient sign method is generated as

$$X_0^{adv} = X,$$

$$X_{N+1}^{adv} = \text{Clip}_{X, \epsilon} \{X_N^{adv} - \alpha \text{sign}(\nabla_X J(X_N^{adv}, y_t))\}$$

where $\text{Clip}_{X, \epsilon} \{X'\}$ represents a clipping of the values of the adversarial example. So the results are within ϵ -neighbourhood of the input image X . This

attack approach is more powerful because the attacker can control how far the adversarial example past the classification boundary.

In our experiments we use $\alpha = 1$ to ensure that we change each pixel by 1 on each step. And we use $\epsilon \leq 8$ because such perturbations that are only perceived as a small noise can create a large number of adversarial examples classified as the desired class by the trained network. It was shown that the attack of iterative gradient sign method was better than FGSM on ImageNet-1000 [19].

2.1.3. Deepfool

Deepfool is an untargeted attack method to generate an adversarial example by iteratively perturbing an image [11]. This method explores the nearest decision boundary. It is assumed that DNN is linear with hyperplanar decision boundary because it is usually hard to solve this problem directly. The image is modified a little to reach the boundary in each iteration. The algorithm stops once the image changes the classification of the network. We apply the powerful l_2 version of Deepfool.

2.1.4. Carlini & Wagner (CEW)

Carlini & Wagner introduced a white-box attack method to generate adversarial examples with small perturbation [12]. The attack can be targeted or untargeted. This attack method has three metrics to measure its distortion (l_0 , l_2 , l_∞). We introduce the main idea of the untargeted l_2 version which has the best performance. It generates adversarial examples by solving the following optimization problem:

$$\begin{aligned} & \underset{\delta}{\text{minimize}} \quad \|\delta\|_2 + c \cdot f(x + \delta) \\ & \text{s.t.} \quad x + \delta \in [0, 1]^n \end{aligned}$$

This attack is to look for the smallest perturbation measured by l_2 norm and make the network classify the image incorrectly at the same time. c is a hyperparameter to balance the two. $f(x)$ is the loss function to measure the

distance between the input image and the adversarial image. $f(x)$ is defined as:

$$f(x) = \max(Z(x)_{true} - \max_{i \neq true} \{Z(x)_i\}, -\kappa)$$

$Z(x)$ is the pre-softmax classification result vector. κ is a hyper-parameter called confidence. High-confidence attacks often have larger perturbation and better transferability to other models.

2.2. Defenses

2.2.1. Adversarial training

Adversarial training is to train a better network by using a mixture of normal and adversarial examples in the training set for data augmentation, which we refer to as adversarial training [8]. In this way, the network learns the features from normal and adversarial examples and can classify adversarial examples correctly. However, it is hard to reason about what attacks to train on and how important the adversarial component should be.

2.2.2. Preprocessing the input

This method preprocesses all the input images before classification to eliminate adversarial perturbations. Adversarial examples may be recovered to the original class after preprocessed. This method usually has good performance when the adversarial examples are not very robust in spatial domain. There are many operations to remove adversarial perturbations, such as principal component analysis [20], JPEG compression [21], adding noise, cropping, rotating and so on. In addition, some researchers recover the adversarial example to the original class by using autoencoders or adding a subnet to the classifier.

2.2.3. Defensive distillation

Defensive distillation is a strong defense method which trains a robust network and it is nearly impossible for gradient based attacks to generate adversarial examples directly on it [15]. Defensive distillation hides the gradient between the pre-softmax layer and softmax outputs by leveraging distillation training

techniques. However, Carlini & Wagner showed that defensive distillation can be attacked by adopting one of the three following strategies: (1) choose a more proper loss function (2) calculate gradient directly from pre-softmax layer instead of from post-softmax layer (3) attack an easy-to-attack network first and then transfer to the distilled network.

2.2.4. Detecting adversarial examples

There are several researches which focus on detecting adversarial examples [17], [18], [22]. All the input images are detected by a detector before feeding them into the network. The detector is a binary classifier to distinguish whether the input image is an adversarial example or not. Although this defense mechanism can not directly classify the adversarial example into the correct class, it can be combined with the above defense methods. If the input image is detected to be an adversarial example, we use the above defense methods to get its correct class. If the input image is detected to be normal example, we feed it into the original network to get its true class. In this way, the total accuracy of classifying input images is increased.

3. Detector

Assuming that we have known the attacking method used by the attacker, we construct a detector to detect whether the input image is an adversarial example or not. Our detecting model exploits the independence of the adversarial perturbation. By modeling the deviations between neighboring pixels in normal images, our detecting method identifies differences from this model and supposes that such differences are due to adversarial attacks. In the beginning, we use a filter to suppress the content of the input image. Dependence between adjacent pixels of the filtered image is modeled as a higher order Markov chain [23]. Then the transition probability matrix is used as a vector feature for a feature based detector implemented using machine learning algorithms.

3.1. Estimation of Modification Weight Map

Considering the perturbation of adversarial examples is in the spatial domain of the original images, we try to estimate the location of modification region of each input image before detecting. Without loss of generalization, we take Fast Gradient Sign Method for example. Assuming that I is an (m, n) image with a range of $[0, 255]$ of pixel values, we denote the value of the gradient of pixel $I_{i,j}$ as $grad_{i,j}$, the weight of pixel $I_{i,j}$ as $W_{i,j}$, and $i \in \{1, \dots, m\}$, $j \in \{1, \dots, n\}$. Although we do not know whether the input image is an adversarial example or not, we can randomly select L categories from the network and use the input image to generate L targeted adversarial examples. When generating the p -th adversarial examples of the input image, we save absolute values of the gradient of each pixel, and then normalize them to $(0, 1)$ to obtain the gradient map $Grad(p)$ from the p -th adversarial example, and $p \in (1, \dots, L)$. We denote the value of the p -th gradient map of pixel $I_{i,j}$ as $Grad(p)_{i,j}$. This leads to

$$Grad(p)_{i,j} = \frac{\left| grad(p)_{i,j} \right| - \min \left\{ \left| grad(p)_{i,j} \right| \right\}}{\max \left\{ \left| grad(p)_{i,j} \right| \right\} - \min \left\{ \left| grad(p)_{i,j} \right| \right\}}$$

Finally, the gradient maps of L adversarial examples are added up and then normalized to $(1, 2)$ to get the modification weight map of each input image. So we can calculate the weight $W_{i,j}$ of pixel $I_{i,j}$ in this way:

$$W_{i,j} = 1 + \frac{1}{L} \sum_{p=1}^L Grad(p)_{i,j}$$

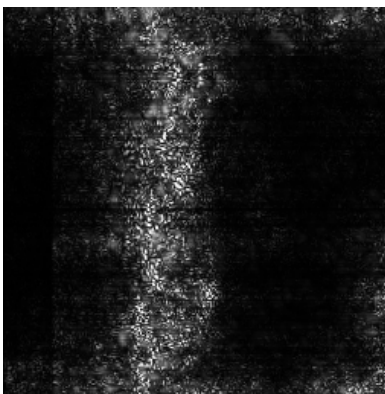
The pixel with larger weight tends to have larger probability to be modified when generating adversarial examples. The results of our experiments show that the modification weight maps of one normal image and its adversarial images are quite similar. Figure 2 shows an example of a normal image, an adversarial image and their modification weight maps (normalized to $(0, 255)$ to show more clearly).

3.2. Construction of Detector

The detecting model is described as follows. First, the model calculates the transition probabilities between pixels in eight directions $\{\leftarrow, \rightarrow, \downarrow, \uparrow, \swarrow, \searrow, \nearrow, \nwarrow\}$



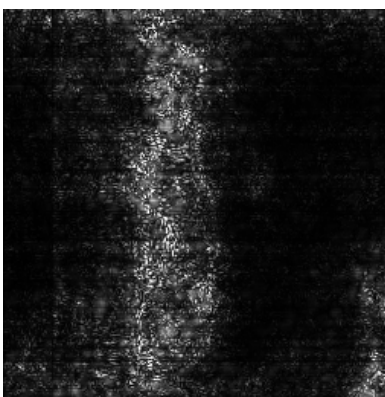
(a) Normal image



(b) Modification weight map of normal image



(c) Adversarial image



(d) Modification weight map of adversarial image

Figure 2: Illustrations of normal image, adversarial image and their modification weight maps

in the spatial domain. The differences and the transition probability are always computed along the same direction. For example, the horizontal direction from left-to-right differences are calculated by $A_{i,j}^{\rightarrow} = I_{i,j} - I_{i,j+1}$, where I is an (m, n) image, and $i \in \{1, \dots, m\}$, $j \in \{1, \dots, n-1\}$. Second, to model pixel dependence along the eight directions, a Markov chain is used between pairs of differences (first order chain) or triplets (second order chain). The first-order detecting features, F^{1st} , model the difference arrays A by a first-order Markov process. For the horizontal direction, this leads to

$$M_{x,y}^{\rightarrow} = P(A_{i,j+1}^{\rightarrow} = x | A_{i,j}^{\rightarrow} = y)$$

where $x, y \in \{-T, \dots, T\}$. Considering the impact of the Modification Weight Map, we try to construct a new Markov transition probability based on Modification Weight Map. The Markov transition probability $M_{x,y}^{\rightarrow}$ is related to the pixel $I_{i,j}$, $I_{i,j+1}$ and $I_{i,j+2}$. So we calculate the new Markov transition probability $M_{x,y}^{\prime\rightarrow}$ in this way:

$$M_{x,y}^{\prime\rightarrow} = M_{x,y}^{\rightarrow} \cdot W_{i,j} \cdot W_{i,j+1} \cdot W_{i,j+2}$$

The second-order detecting features, F^{2nd} , model the difference arrays A by a second-order Markov process. For the horizontal direction, this leads to

$$M_{x,y,z}^{\rightarrow} = P(A_{i,j+2}^{\rightarrow} = x | A_{i,j+1}^{\rightarrow} = y, A_{i,j}^{\rightarrow} = z)$$

where $x, y, z \in \{-T, \dots, T\}$. Similarly, the new Markov transition probability $M_{x,y,z}^{\prime\rightarrow}$ is

$$M_{x,y,z}^{\prime\rightarrow} = M_{x,y,z}^{\rightarrow} \cdot W_{i,j} \cdot W_{i,j+1} \cdot W_{i,j+2} \cdot W_{i,j+3}$$

For dimensionality reduction of the transition probability matrix, only differences within a limited range are considered. Thus, the transition probability matrix is calculated just for pairs within $[-T, T]$. We separately average the horizontal and vertical matrices and then the diagonal matrices to form the final feature sets, F^{1st} , F^{2nd} . The expression of the average sample Markov transition probability matrices is

$$F_{1,\dots,k} = (M^{\rightarrow} + M^{\leftarrow} + M^{\uparrow} + M^{\downarrow})/4$$

$$F_{k+1,\dots,2k} = (M'^{\nearrow} + M'^{\swarrow} + M'^{\searrow} + M'^{\nwarrow})/4$$

where $k = (2T + 1)^2$ for the first-order detecting features and $k = (2T + 1)^3$ for the second-order detecting features. We can see that the order of Markov model and the range of differences T control the dimensionality of our detecting model. We use $T = 3$ for second order, resulting in $2k = 686$ features [24].

The construction of our detector based on detecting features relies on pattern-recognition classifiers. The detectors were trained as binary classifiers implemented using the FLD ensemble [25] with default settings. As described in the original publication, the ensemble by default minimizes the total classification error probability under equal priors $P_E = \min_{P_{FA}} (P_{FA} + P_{MD})/2$, where P_{FA} and P_{MD} are the false-alarm of missed-detection probabilities. The random subspace dimensionality and the number of base learners is found by minimizing the out-of-bag (OOB) estimate of the testing error, E_{OOB} , on bootstrap samples of the training set as it is an unbiased estimate of the testing error on unseen data [26].

To prove that Modification Weight Map is effective when detecting adversarial examples, we perform a comparative experiment. We use the above algorithm to construct two detectors. The only difference of them is one detector with Modification Weight Map and the other detector without Modification Weight Map, that is to say, the other detector’s modification weight of each pixel is set to 1. We use these two detectors to detect the same adversarial examples and compare their adversarial detection accuracy. We can see from Figure 3 and Figure 4 that the detector with Modification Weight Map has higher adversarial detection accuracy.

4. Experiments and Results

We construct the detector by modeling the differences between adjacent pixels in natural images. Therefore, our method can not achieve very good performance on MNIST and CIFAR-10 because the size of the image is too small. However, it has good performance on ImageNet-1000. Our experiments are

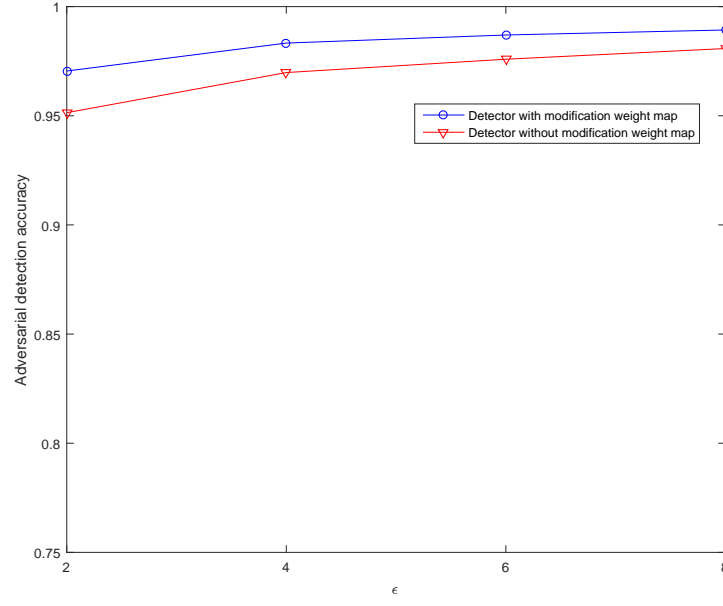


Figure 3: Effectiveness of Modification Weight Map detecting targeted adversarial images generated by fast gradient sign method.

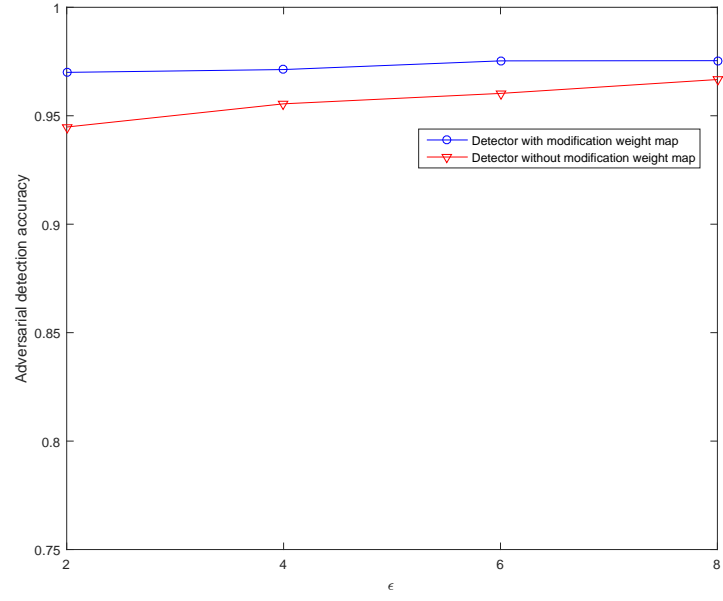


Figure 4: Effectiveness of Modification Weight Map detecting targeted adversarial images generated by iterative gradient sign method.

performed on 40000 images randomly selected from ImageNet-1000 (ILSVRC-2016) using a pretrained VGG-16 model [27] as classification network which is evaluated with top-1 accuracy. This results in a train set of 25000 images, a validation set of 5000 images, and a test set of 10000 images. The format of these 40000 clean images is JPEG. We divide adversarial attacks into two types. In targeted attack, the attacker generates adversarial examples which the classifier misclassify into a particular class. In untargeted attack, the attacker generates adversarial examples which the classifier misclassify into any class as long as it is different from the true class. We test our detecting method against attacks using fast gradient sign method, iterative gradient sign method, Deepfool and Carlini’s method. The detector is trained and tested on the same adversarial method.

4.1. Detecting Targeted Adversarial Examples

We test our detecting method against targeted attacks using fast gradient sign method, iterative gradient sign method and Carlini’s method. At first, these 40000 images are classified by the network to obtain their true labels. Then we use these 40000 images to generate 40000 adversarial images as adversarial samples of our experiments. Table 1 and Table 2 illustrate the generalizability of trained detectors for the same adversary with different choices of ϵ . While a detector trained for large ϵ does not generalize very well to small ϵ , the other direction works reasonably well. Please note that these values of ϵ are based on assuming a range of $[0, 255]$ per color channel of the input. The results of detecting targeted adversarial examples generated by Carlini’s method is shown in Table 3.

We compare our detecting method with the Binarized RBF-SVM detector [18]. The results of detecting targeted adversarial examples by the Binarized RBF-SVM detector is shown in Table 4 and Table 5.

4.2. Detecting Untargeted Adversarial Examples

Previous work showed that untargeted attack is easier to succeed, results in smaller perturbations, and transfers better to different models. So we also detect

Table 1: Detect targeted adversarial images generated by fast gradient sign method.

FGSM	normal images	$\varepsilon_{test} = 2$	$\varepsilon_{test} = 4$	$\varepsilon_{test} = 6$	$\varepsilon_{test} = 8$
$\varepsilon_{train} = 2$	0.9730	0.9705	0.9738	0.9689	0.9643
$\varepsilon_{train} = 4$	0.9860	0.5327	0.9833	0.9852	0.9849
$\varepsilon_{train} = 6$	0.9912	0.2454	0.9789	0.9870	0.9980
$\varepsilon_{train} = 8$	0.9930	0.1756	0.9653	0.9867	0.9893

Table 2: Detect targeted adversarial images generated by iterative gradient sign method.

IGSM	normal images	$\varepsilon_{test} = 2$	$\varepsilon_{test} = 4$	$\varepsilon_{test} = 6$	$\varepsilon_{test} = 8$
$\varepsilon_{train} = 2$	0.9703	0.9700	0.9656	0.9419	0.9191
$\varepsilon_{train} = 4$	0.9729	0.9544	0.9713	0.9694	0.9627
$\varepsilon_{train} = 6$	0.9754	0.6734	0.9579	0.9753	0.9750
$\varepsilon_{train} = 8$	0.9757	0.4028	0.9066	0.9733	0.9754

Table 3: Detect targeted adversarial images generated by Carlini's method.

C&W	normal images	adversarial examples
l_2	0.7369	0.7182

Table 4: Binarized RBF-SVM detector detects targeted adversarial images generated by fast gradient sign method and iterative gradient sign method.

FGSM	$\epsilon = 2$	$\epsilon = 4$	$\epsilon = 6$	$\epsilon = 8$
	0.8371	0.9080	0.9437	0.9655
IGSM	$\epsilon = 2$	$\epsilon = 4$	$\epsilon = 6$	$\epsilon = 8$
	0.8259	0.8842	0.9148	0.9485

Table 5: Binarized RBF-SVM detector detects targeted adversarial images generated by Carlini's method.

C&W	normal images	adversarial examples
l_2	0.5623	0.5482

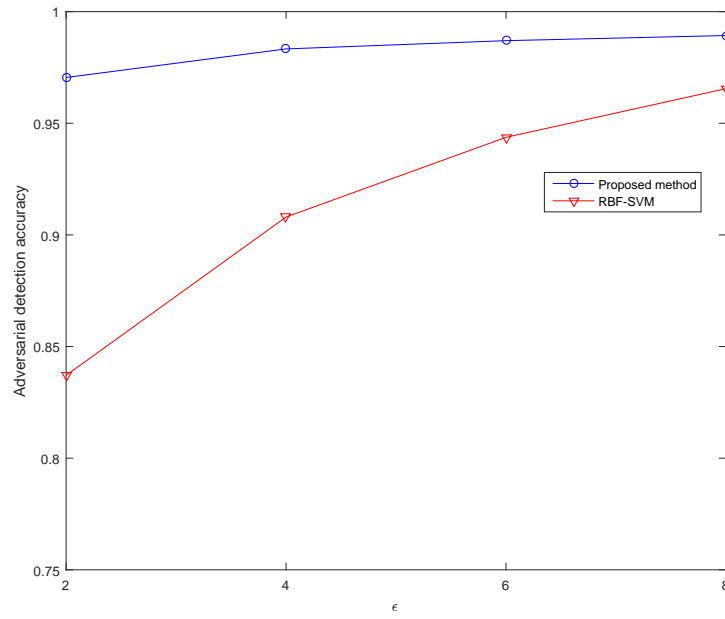


Figure 5: Results for detecting targeted adversarial images generated by fast gradient sign method.

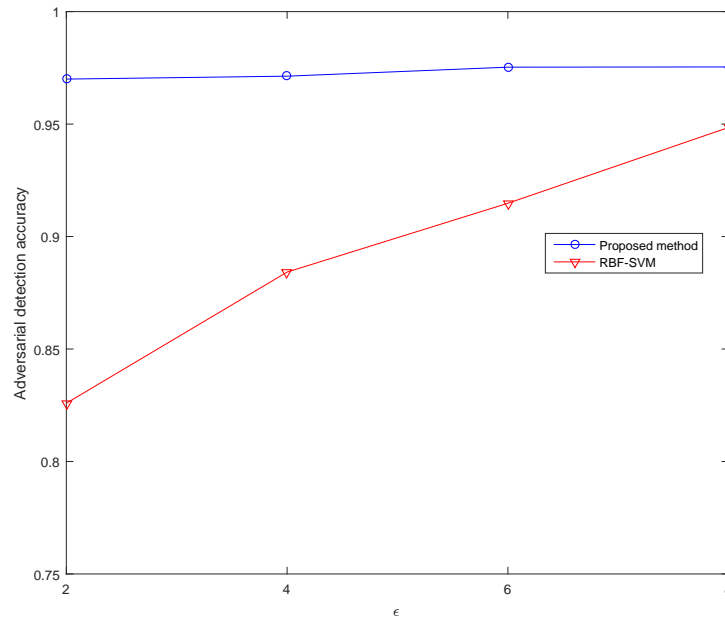


Figure 6: Results for detecting targeted adversarial images generated by iterative gradient sign method.

untargeted adversarial examples to see the performance of our method. The steps of experiments are similar with detecting targeted adversarial examples. The only difference is that we use untargeted adversarial examples to train the detector. We test our detecting method against attacks using fast gradient sign method, iterative gradient sign method, Deepfool and Carlini’s method. The results of detecting targeted adversarial examples are shown in Table 6, Table 7 and Table 8. We also compare our detecting method with the Binarized RBF-SVM detector. The results of detecting untargeted adversarial examples by the Binarized RBF-SVM detector is shown in Table 9 and Table 10.

Table 6: Detect untargeted adversarial images generated by fast gradient sign method.

FGSM	normal images	$\varepsilon_{test} = 2$	$\varepsilon_{test} = 4$	$\varepsilon_{test} = 6$	$\varepsilon_{test} = 8$
$\varepsilon_{train} = 2$	0.9725	0.9704	0.9687	0.9663	0.9619
$\varepsilon_{train} = 4$	0.9758	0.6258	0.9719	0.9638	0.9576
$\varepsilon_{train} = 6$	0.9812	0.5303	0.9640	0.9751	0.9657
$\varepsilon_{train} = 8$	0.9868	0.3916	0.9589	0.9637	0.9806

Table 7: Detect untargeted adversarial images generated by iterative gradient sign method.

IGSM	normal images	$\varepsilon_{test} = 2$	$\varepsilon_{test} = 4$	$\varepsilon_{test} = 6$	$\varepsilon_{test} = 8$
$\varepsilon_{train} = 2$	0.9708	0.9638	0.9371	0.8895	0.7916
$\varepsilon_{train} = 4$	0.9737	0.7189	0.9675	0.9643	0.9548
$\varepsilon_{train} = 6$	0.9749	0.3620	0.9611	0.9725	0.9730
$\varepsilon_{train} = 8$	0.9760	0.3211	0.9565	0.9737	0.9745

Table 8: Detect untargeted adversarial images generated by Deepfool and Carlini’s method.

Deepfool	normal images	adversarial examples
l_2	0.9289	0.9186
C&W	normal images	adversarial examples
l_2	0.6957	0.6778

Table 9: Binarized RBF-SVM detector detects untargeted adversarial images generated by fast gradient sign method and iterative gradient sign method.

FGSM	$\epsilon = 2$	$\epsilon = 4$	$\epsilon = 6$	$\epsilon = 8$
	0.8258	0.8936	0.9243	0.9541
IGSM	$\epsilon = 2$	$\epsilon = 4$	$\epsilon = 6$	$\epsilon = 8$
	0.7975	0.8752	0.9072	0.9330

Table 10: Binarized RBF-SVM detector detects untargeted adversarial images generated by Deepfool and Carlini’s method.

Deepfool	normal images	adversarial examples
l_2	0.7395	0.7534
C&W	normal images	adversarial examples
l_2	0.5332	0.5187

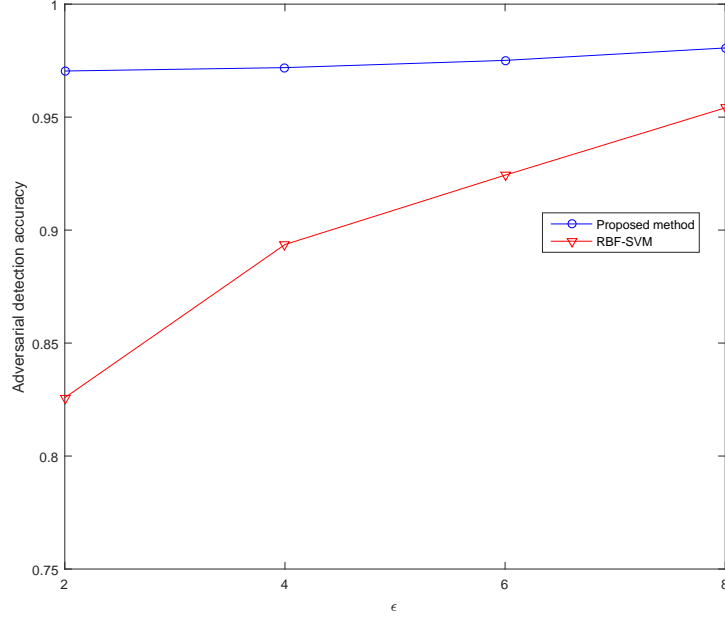


Figure 7: Results for detecting untargeted adversarial images generated by fast gradient sign method.

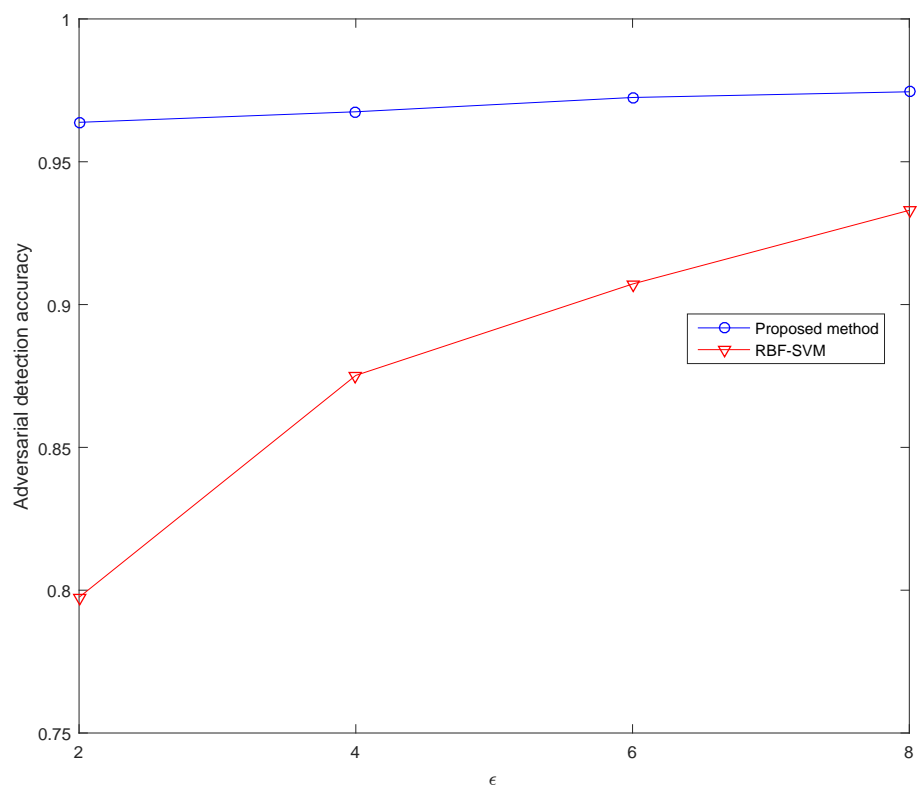


Figure 8: Results for detecting untargeted adversarial images generated by iterative gradient sign method.

According to the results of the experiment, our detecting method can correctly distinguish normal images and adversarial images when the detector is trained and tested on the same adversarial method in most cases. However, the performance of our detection model is not good enough against Carlini’s method. In addition, the detector trained for $\epsilon = 2$ generalizes well to large ϵ when detecting adversarial examples generated by fast gradient sign method and iterative gradient sign method.

5. Conclusions and Future Work

In this paper, we have shown that adversarial examples can be effectively detected with the detector based on steganalysis. Our experiments are performed on ImageNet-1000 using VGG-16 network. This simulates the problem of object classification in real scenes. Although we have only performed experiments on one network, it is believed that our method can be extended to other network structures. However, our detector can’t have very good performance when it is not trained and tested on the same adversarial method. In future work, we will try to explore methods for training one detector against different kinds of adversarial attacks.

Acknowledgments

This work was supported in part by the Natural Science Foundation of China under Grants U1636201 and 61572452. Jiayang Liu, Weiming Zhang, Yiwei Zhang, Dongdong Hou, Yujia Liu and Nenghai Yu are with CAS Key Laboratory of Electromagnetic Space Information, University of Science and Technology of China, Hefei 230026, China.

References

References

- [1] O. Russakovsky, J. Deng, H. Su, J. Krause, S. Satheesh, S. Ma, Z. Huang, A. Karpathy, A. Khosla, M. Bernstein, et al., Imagenet large scale visual

- recognition challenge, *International Journal of Computer Vision* 115 (3) (2015) 211–252.
- [2] K. He, X. Zhang, S. Ren, J. Sun, Deep residual learning for image recognition, in: *Proceedings of the IEEE Conference on Computer Vision and Pattern Recognition*, 2016, pp. 770–778.
 - [3] D. Amodei, R. Anubhai, E. Battenberg, C. Case, J. Casper, B. Catanzaro, J. Chen, M. Chrzanowski, A. Coates, G. Diamos, et al., Deep speech 2: End-to-end speech recognition in english and mandarin, in: *International Conference on Machine Learning*, 2016, pp. 173–182.
 - [4] J. Yu, B. Zhang, Z. Kuang, D. Lin, J. Fan, iprivacy: image privacy protection by identifying sensitive objects via deep multi-task learning, *IEEE Transactions on Information Forensics and Security* 12 (5) (2017) 1005–1016.
 - [5] A. Frome, G. Cheung, A. Abdulkader, M. Zennaro, B. Wu, A. Bissacco, H. Adam, H. Neven, L. Vincent, Large-scale privacy protection in google street view, in: *Computer Vision, 2009 IEEE 12th International Conference on*, IEEE, 2009, pp. 2373–2380.
 - [6] G. E. Dahl, J. W. Stokes, L. Deng, D. Yu, Large-scale malware classification using random projections and neural networks, in: *Acoustics, Speech and Signal Processing (ICASSP)*, 2013 IEEE International Conference on, IEEE, 2013, pp. 3422–3426.
 - [7] C. Szegedy, W. Zaremba, I. Sutskever, J. Bruna, D. Erhan, I. Goodfellow, R. Fergus, Intriguing properties of neural networks, *International Conference on Learning Representations*.
 - [8] I. J. Goodfellow, J. Shlens, C. Szegedy, Explaining and harnessing adversarial examples, *International Conference on Learning Representations*.

- [9] A. Rozsa, E. M. Rudd, T. E. Boulton, Adversarial diversity and hard positive generation, in: *Computer Vision and Pattern Recognition Workshops*, 2016, pp. 410–417.
- [10] N. Papernot, P. McDaniel, S. Jha, M. Fredrikson, Z. B. Celik, A. Swami, The limitations of deep learning in adversarial settings, in: *IEEE European Symposium on Security and Privacy*, 2016, pp. 372–387.
- [11] S. M. Moosavidezfooli, A. Fawzi, P. Frossard, Deepfool: A simple and accurate method to fool deep neural networks, in: *Computer Vision and Pattern Recognition*, 2015, pp. 2574–2582.
- [12] N. Carlini, D. Wagner, Towards evaluating the robustness of neural networks, in: *Security and Privacy*, 2017.
- [13] S. Gu, L. Rigazio, Towards deep neural network architectures robust to adversarial examples, *International Conference on Learning Representations*.
- [14] S. Zheng, Y. Song, T. Leung, I. Goodfellow, Improving the robustness of deep neural networks via stability training, in: *Proceedings of the IEEE Conference on Computer Vision and Pattern Recognition*, 2016, pp. 4480–4488.
- [15] N. Papernot, P. McDaniel, X. Wu, S. Jha, A. Swami, Distillation as a defense to adversarial perturbations against deep neural networks, in: *Security and Privacy (SP), 2016 IEEE Symposium on*, IEEE, 2016, pp. 582–597.
- [16] A. Rozsa, M. Günther, T. E. Boulton, Are accuracy and robustness correlated?, *International Conference on Machine Learning and Applications*.
- [17] J. H. Metzen, T. Genewein, V. Fischer, B. Bischoff, On detecting adversarial perturbations, *International Conference on Learning Representations*.
- [18] J. Lu, T. Issaranon, D. Forsyth, Safetynet: Detecting and rejecting adversarial examples robustly, in: *IEEE International Conference on Computer Vision*, 2017, pp. 446–454.

- [19] A. Kurakin, I. Goodfellow, S. Bengio, Adversarial examples in the physical world, International Conference on Learning Representations.
- [20] A. N. Bhagoji, D. Cullina, P. Mittal, Dimensionality reduction as a defense against evasion attacks on machine learning classifiers, arXiv preprint arXiv:1704.02654.
- [21] N. Das, M. Shanbhogue, S.-T. Chen, F. Hohman, L. Chen, M. E. Kounavis, D. H. Chau, Keeping the bad guys out: Protecting and vaccinating deep learning with jpeg compression, arXiv preprint arXiv:1705.02900.
- [22] D. Meng, H. Chen, Magnet: a two-pronged defense against adversarial examples, in: Proceedings of the 2017 ACM SIGSAC Conference on Computer and Communications Security, ACM, 2017, pp. 135–147.
- [23] K. Sullivan, U. Madhow, S. Chandrasekaran, B. S. Manjunath, Steganalysis of spread spectrum data hiding exploiting cover memory, in: Electronic Imaging 2005, International Society for Optics and Photonics, 2005, pp. 38–46.
- [24] T. Pevny, P. Bas, J. Fridrich, Steganalysis by subtractive pixel adjacency matrix, IEEE Transactions on information Forensics and Security 5 (2) (2010) 215–224.
- [25] J. Kodovsky, J. Fridrich, V. Holub, Ensemble classifiers for steganalysis of digital media, IEEE Transactions on Information Forensics and Security 7 (2) (2012) 432–444.
- [26] L. Breiman, Bagging predictors, Machine learning 24 (2) (1996) 123–140.
- [27] K. Simonyan, A. Zisserman, Very deep convolutional networks for large-scale image recognition, Computer Science.